Effective Wastewater Treatment using Advanced Oxidation Process Combined with Magnetic Nanoparticle Setup

Ihab H. Alsurakji[1,*], Amjad El-Qanni[2,*], Emad Salahat[1], Abdelkareem Arman[1], Mohammad Abuabiah[3], Waleed Abuzaina[3]

[1] An-Najah National University, Department of Mechanical Engineering, Nablus 7, Palestine;
[2] An-Najah National University, Department of Chemical Engineering, Nablus 7, Palestine;
[3] An-Najah National University, Department of Mechatronics Engineering, Nablus 7, Palestine;

[*]*Corresponding authors: isurakji@najah.edu; Tel.: +97059581448; a.elqanni@najah.edu; Tel.: +970594545128;*

Abstract: Industrial organic wastewater effluents affect our ecosystem, especially when discharged without any treatment. Nowadays, advanced oxidation process (AOP) is considered one of the most conventional treatment techniques. It mainly depends on producing hydroxyl radicals (·OH) in presence of an oxidizing agent and/or bulk or nanoparticles which must have high sorption affinity and photocatalytic activity to speed up the treatment process. In this study, a magnetic iron oxide (Fe_3O_4) nanoparticle was used along with hydrogen peroxide (H_2O_2) and sodium persulfate ($Na_2S_2O_8$) for comparison purposes. This magnetic nanoparticle (MN) has a high surface-area-to-volume ratio and is magnetic in nature which can be recovered by a magnetic field for further cycles of treatment and regeneration once needed. To the best of our knowledge, there is no continuous industrial process for such a treatment. Thus, a bench-scale setup that provides continuous wastewater flow was built which mainly depends on using four stages mechanism and recovering MN using the magnetic field. This study should help in quantifying the efficiency, performance, and give insights regarding its feasibility towards wastewater treatment on an industrial scale. Hence, design and automated controlling parameters, optimal operating conditions, and economical descriptions were addressed in this work.

Keywords: Advanced oxidation process (AOP); sodium persulfate ($Na_2S_2O_8$); hydrogen peroxide (H_2O_2); magnetic nanoparticle (MN); (Fe_3O_4) nanoparticle material; chemical oxygen demand (COD).

1. Introduction

The global population and industrial sectors are increasing rapidly nowadays, therefore solid waste and wastewater effluents are dramatically increasing. Therefore, residential building wastes must be considered through population growth. Hence, environmental institutions and governmental organizations shall constitute laws that restrict effluent resources by limiting their discharge, and by treating domestic and industrial wastewater. Generally, the sources of such effluents come from hospital discharges, landfill leachates, slaughterhouses, textile industry, livestock, and aquaculture [1-4]. Remarkably, those effluents are rich in chemical, colors, organic pollutants, and dyestuffs [5]. For instance, slaughterhouse wastewater effluents are a vital source of colored wastewater. The Palestinian Central Bureau of Statistics (PCBS) found that 17 slaughterhouses in Palestine; 11 in the West Bank and 6 in the Gaza Strip [6]. Thus, pollution prevention, solid waste management, and wastewater treatment are a must in Palestine to keep a clean and sustainable environment.

One of the most effective processes for treating wastewater is the advanced oxidation process (AOP), with the principle of oxidizing most of the organic pollutants. This technology has a conventional method for treating through producing hydroxyl radicals ($^{\cdot}OH$) that attack the organic pollutants or sulfate radical-based AOPs which are sufficient for degrading refractory organic pollutants. Moreover, $^{\cdot}OH$ can be gained using hydrogen peroxide (H_2O_2) along with other metal oxide-based catalysts that speed up the reaction rate of AOP [1, 7].

There are different treatment techniques used in AOPs. For instance, Fenton technique, which depends on producing $^{\cdot}OH$ removal from the reaction of (H_2O_2) with iron-based catalyst, since this mixture between Fe^{+2} and H_2O_2 is called Fenton's reagent [8], and the chemical reactions that represent $^{\cdot}OH$ are:

$$Fe^{+2} + H_2O_2 \rightarrow Fe^{+3} + HO^- + HO^{\cdot} \quad (1)$$

$$Fe^{+3} + H_2O_2 \rightarrow Fe^{+2} + FeOOH^{+2} \quad (2)$$

$$FeOOH^{+2} \rightarrow OH_2^{\cdot} + Fe^{+2} \quad (3)$$

Nanoparticle technology is emerging as one of the most interesting technologies for enhancing wastewater treatment. Literature review reveals that metal-oxide-based nanoparticles have unique properties in comparison with their counter parts for energy and environmental applications [9-12]. Owing to their nano-size, exceptional high. surface area to volume ratio, and easily manipulated surface make nanoparticles suitable as nanoadsorbents and nanocatalysts [13]. However, one of the critical challenges for this technology is the use of nanoparticles in continuous modes. Herein, in this study the investigation of the use of magnetic iron oxide nanoparticles, magnetite (Fe_3O_4) for degrading synthetic wastewater exemplified by crystal violet (CV) model molecule within a continuous in-house prototype. In addition, two different oxidation agents, hydrogen peroxide (H_2O_2) and sodium persulfate ($Na_2S_2O_8$), were also used to mimic the AOP process and to compare their degradation degree of CV model molecule at different initial concentration. At the end, optimal design parameters were estimated to give a comprehensive process description and thus promote its feasibility.

2. Materials and Methods

2.1. Dye model molecule

Synthetic wastewater samples were prepared using a crystal violet (CV) model dye molecule which could mimic colored and textile wastewater effluents [5]. This molecule has been purchased from Sigma-Aldrich and used without any further treatment. Table 1 and Figure 1 show the CV dye properties and its structure, respectively.

Table 1. Crystal violet model molecule properties.

Items	Specifications
Chemical formula	$C_{25}N_3H_{30}CL$
Molecular weight (MW)	407.98 $g.mol^{-1}$
Max wavelength (λ_{max})	590 nm
Purity	98%

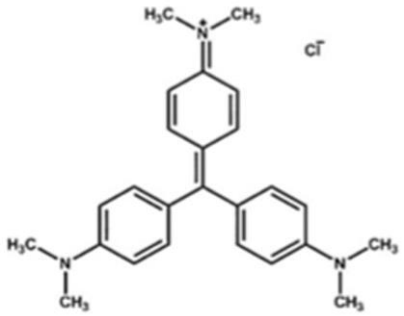

Figure 1. Crystal violet chemical structure [5].

A stock of 200 ppm of CV dye solution was prepared by dissolving a specified amount of CV in 20 mL of deionized water (DW) and subsequently diluted to the required concentration; 30 ppm. The concentration of 200 ppm dye was prepared by using the following equation:

$$\mathrm{C} = \frac{\mathrm{m}}{\mathrm{pu} \times \mathrm{V}} \tag{4}$$

where C is the CV dye concentration (ppm), pu is the purity of the CV dye, m is the desired mass of the CV dye (mg), and V is the volume of the DW (L). Applying equation 4 yields the desired mass of CV dye which is equal to ~ 4.0 mg which means diluting 4.0 mg of the CV dye with 0.02 L of DW producing 200 ppm CV dye concentration. The dilution equation can be described as:

$$\mathrm{V_1\ M_1\ =\ V_2\ M_2} \tag{5}$$

where $\mathrm{V_1}$ is the volume needs to be diluted (L), $\mathrm{M_1}$is the dye concentration before dilution (ppm), $\mathrm{V_2}$ is the desired volume (L) which is equal to 0.02 L, and $\mathrm{M_2}$ is the desired CV dye concentration (ppm) which is equal to 30 ppm. Applying equation 5, yields $\mathrm{V_1}$ equal to 0.003 L which means using 0.003 L from the 200 ppm CV dye solution and adding 0.017 L DW producing a dye solution with concentration of 30 ppm and volume of 0.02 L.

To determine the calibration curve of UV-Vis absorbance of CV concentration, the absorbance of the CV aqueous solution at different known concentrations was determined using UV-Vis spectrophotometry (Genesys 10S, Thermo Scientific Instruments Canada Inc., Mississauga, ON) at a wavelength of 590 nm. Three trials were performed at same ambient room temperature, constant pH which was around 6.0, and different initial concentrations varied from 10 to 30 ppm. A well-fitted regression equation for the calibration curve, $C = 10.582 \times Abs$, was obtained with a linear regression coefficient, $R^2 > 0.99$, where C is the CV concentration in ppm and Abs is the absorbance. Subsequently, the absorbance of the CV aqueous solution that had been degraded after the reaction was measured and the final concentration was calculated using the calibration curve equation.

2.2. Magnetite nanoparticles and oxidation reagents

Commercial magnetite (Fe_3O_4) nanoparticles used in the experiments as well as the oxidation agents are listed in Table 2. Worth mentioning that two different oxidation agents, H_2O_2 and $Na_2S_2O_8$, were used for comparison purposes.

Table 2. List of chemicals and reagents

Chemical/Reagent	Chemical formula	Purity	Vendor
Commercial magnetite	Fe_3O_4	--	Sigma-Aldrich (Haifa) via local sub-vendor BioTech Medical Supplies (Ramallah, Palestine)
Hydrogen peroxide	H_2O_2	30 % (w/w)	
Sodium persulfate	$Na_2S_2O_8$	98 %	

2.3. Optimization of oxidation agent amounts

In real industrial process shaking time and/or reaction residence time is a challenging parameter. Therefore, to optimize the amounts of H_2O_2 and $Na_2S_2O_8$ oxidation agents with mixing time, three runs were conducted by mixing 30 ppm of CV dye solution with Fe_3O_4 nanoparticles and H_2O_2 agent. A shaker device (Grant OLS200 Orbital Shaking Water Bath, Grant Instruments, Cambridge, UK) was used at constant speed of 40 rpm. Other experimental conditions were: pH at around 6.0, constant room temperature, and constant dose of Fe_3O_4 nanoparticles around $0.1g/10mL$ CV dye.

2.4. Optimization of mixing speed

Mixing the dye model molecule with the oxidation agent along with the nanoparticles were investigated using two methods. First one was by using the shaker device (see section 2.3) and the other one was by using four-blades mixing impeller. Four runs were performed to find the optimal mixing type and speed. In a typical run, 30 ppm of CV dye solution mixed with Fe_3O_4 nanoparticles in a ratio of 0.1g/10mL dye at constant pH (~6.0) and H_2O_2 agent amount which was 4mL/10mL dye.

3. Magnetic nanoparticles-assisted setup

Figure 2 shows a schematic diagram of the bench-scale setup that provides continuous wastewater treatment flow and in-house built prototype. It mainly consists of the following; i) one pre-treatment storage cylinder of 1800 *mL* capacity, ii) three cylinders for wastewater treatment of 600 *mL* each, iii) piping system, valves, couplers, pump, magnet, mixers, and bearings, iv) control unit including power supply, motors, boost, Arduino, and relays, v) chemicals including magnetite nanoparticle, H_2O_2, and $Na_2S_2O_8$ agents.

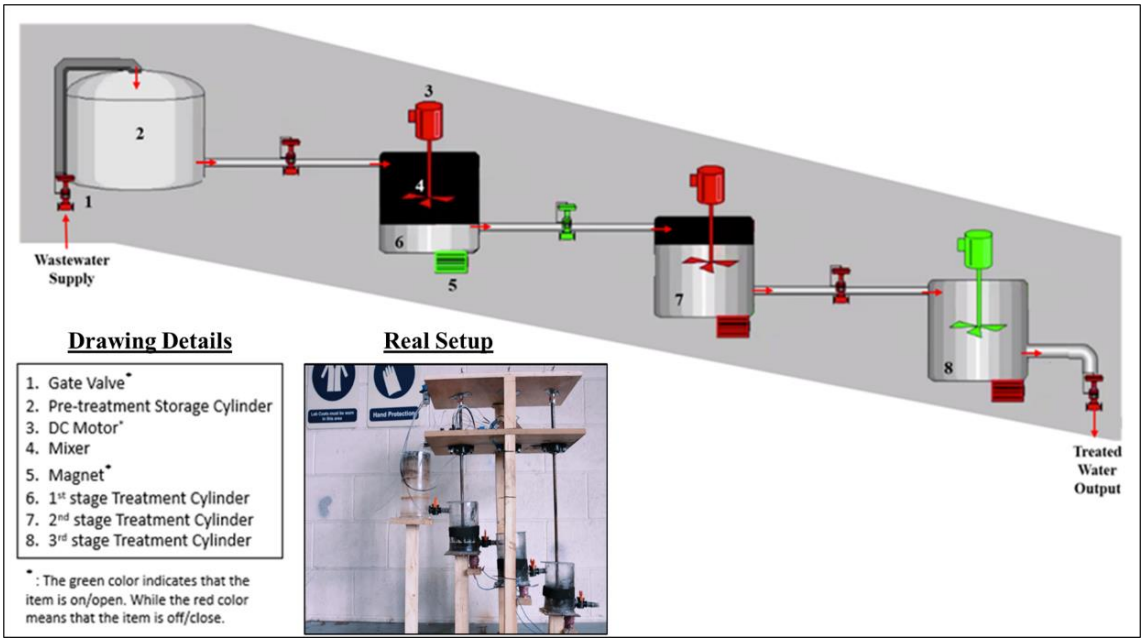

Figure 2. Schematic diagram of the magnetic wastewater treatment setup (drawn by using the Wondershare EdrawMax Software Version 10.5.2) and in-house built prototype.

4. Results and Discussion

4.1. Adsorption along with AOP treatment process

Adsorption and AOP for CV dye model molecule stock solution with different initial concentrations were performed using the in-house built prototype in presence of Fe_3O_4 nanoparticles. Table 3 shows the treatment cycles that were performed by using both oxidation agents H_2O_2 and $Na_2S_2O_8$ alongside the amount of the nanoparticles for each cylinder, the amount of each oxidation agent, the mixing duration, and the initial and final concentrations. The total volume of the prepared dye was 1800 *mL*, and thus 600 *mL* was delivered to each cylinder benefiting from gravity-transfer. As seen, the experimental conditions allowed to fully treat the stock solution of 30-200 ppm of CV, as pure effluents were obtained upon treatment as also shown in Figure 3. However, less amount of $Na_2S_2O_8$ was needed for this process in comparison with H_2O_2. More explanation of this observation will be elaborated in section 4.2.

Table 3. The result of treating of CV dye model molecule solution by using H_2O_2 and $Na_2S_2O_8$ agents.

Agent	Cycle	Amount of Catalyst (g/cylinder)	Amount of Agent (ml/cylinder)	Mixing Time (min/cylinder)	Initial Concentration (ppm)	Final Concentration (ppm)
H_2O_2	1	6	240	10	30	0
	2	6	240	10	30	0
	3	6	240	10	30	0
$Na_2S_2O_8$	1	6	180	10	30	0
	2	6	180	10	30	0
	3	6	180	10	30	0
	1	6	180	10	120	0
	2	6	180	10	120	0
	3	6	180	10	120	0
	1	6	180	10	200	0
	2	6	180	10	200	0
	3	6	180	10	200	0

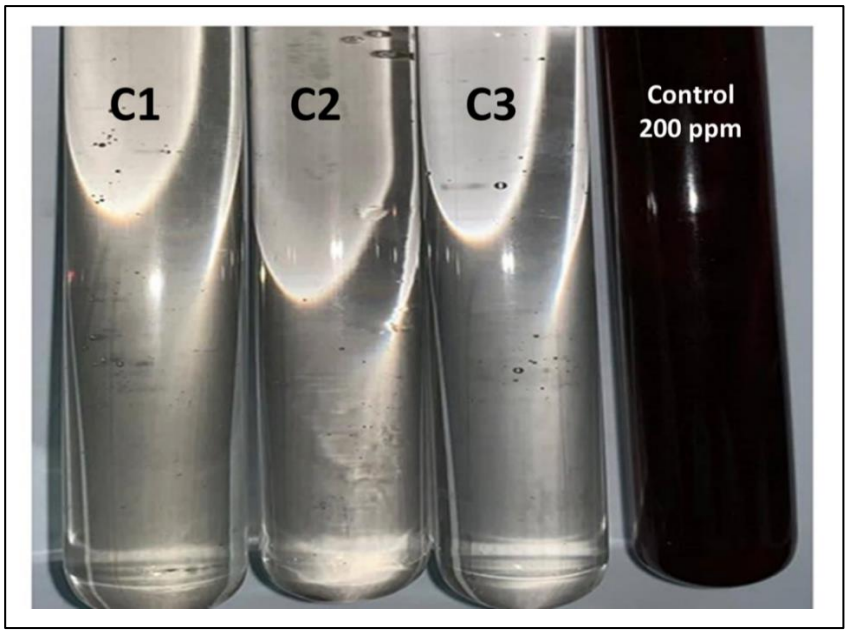

Figure 3. Pure effluents upon treating 200 ppm CV dye model molecule solution using $Na_2S_2O_8$ oxidation agent in presence of Fe_3O_4 nanoparticles.

4.2. Optimal oxidation agent amounts

Table 4 shows the results of the three optimization runs regarding the oxidation agent amounts. As seen, as the amount of H_2O_2 agent is increased the shaking time decreased, as well as the final concentration of the CV dye. The same scenario is noticed for $Na_2S_2O_8$. However, the degradation degree of CV molecule is way bigger in presence of $Na_2S_2O_8$ in comparison with H_2O_2. For instance, the final concentration of CV molecule was dropped to 1.6 ppm and 9.5 ppm in presence of 2 *mL* of $Na_2S_2O_8$ and H_2O_2, respectively. This could be attributed to the stability of each oxidation agent. Since this process is an advanced oxidation process, sulfate-radical-based ($SO_4^{-\bullet}$) is a powerful oxidizing agent than OH-radical-based ($OH^{-\bullet}$). As indicated by Hung et al., 2016, the persulfate anion is thermodynamically more stable than H_2O_2 [14].

Table 4. Optimization results of H_2O_2 and $Na_2S_2O_8$ amounts with mixing time.

Agent	Run	Initial Concentration (ppm)	Amount (mL)	Shaking Time (min)	pH	Final Concentration (ppm)
H_2O_2	1	30	0	60	6	30.0
	2	30	2	60	6	11.2
	3	30	4	30	6	9.5
$Na_2S_2O_8$	1	30	0.5	30	6	4.1
	2	30	1	30	6	1.9
	3	30	2	30	6	1.6

4.3. Optimal mixing speed

This is a vital parameter for the continuous process as the target is to avoid nanoparticles agglomeration as well as the suspension. Thus, Table 5 shows the runs' parameters and the results for optimal mixing type and speed. Noticeably, as the four-blade impeller (conventional mixer) speed increases the final concentration of the dye decreases. As seen, the optimal speed could be in range 300-400 rpm to achieve maximum degradation percentage (64-82 %). Worth mentioning that at this speed range the nanoparticles stayed dispersed neither suspended nor precipitated during the whole time within the experimental runs. Hence, four-blade impeller with a speed of (300-400 rpm) has been chosen for the prototype experiments.

Table 5. The results of optimizing the mixer type and parameters.

Run	Initial Concentration (ppm)	Shaker Speed (rpm)	Four-Blade Impeller Speed (rpm)	Final Concentration (ppm)
1	30	40	--	9.5
2	30	--	200	25.0
3	30	--	300	10.7
4	30	--	400	5.5

4.4. Process Description and Cost estimation

Four 1800 *mL* CV dye samples were prepared at different dye concentrations. Each sample was divided into three 600 *mL* batches passed through three cylinders by using a 16 *mm* ID manual gate valve. The process itself is unique which intended to treat the samples continuously through three stages. A hydrostatic pump of 1.0 *mL/sec* capacity is used for pumping the wastewater effluent into the pre-treatment storage cylinder. Each of the other three cylinders contained a mixer (four-blade impeller) which is used for mixing the sample with 6.0 *g* of Fe_3O_4 nanoparticles for 10 *min*. Initially, the first gate valve between the pre-treatment storage cylinder and the first cylinder is fully opened until a quantity of 600 *mL* is transferred. Then, 10 *min* mixing is conducted for the wastewater and the nanoparticles. Thereafter, a magnetic mechanism is turned on and all nanoparticles were grasped due to their magnetism characteristics. The grasping process lasts for three minutes while the second gate valve is fully closed. While the magnetic mechanism in the first cylinder is still on, the second gate valve is fully opened. Herein, 600 *mL* is transferred between first cylinder and the second one. Same scenarios are repeated for the second and the third cylinders. Interestingly, the three wastewater treatment cylinders were mounted on a wood stand which was designed in a way that allowed gravity-transferred between stages (Figure 2).

A magnetic mechanism was used for generating an electrical magnetic field in order to attract the Fe_3O_4 nanoparticles from the treated wastewater. It consists of a cupper coil wrapped around a steel rod and connected to a power supply. The electrical magnetic field has a proportional relation with the current value and the coil length. Three runs were performed by using the steel rod which

has length of 7 *cm* and 1.4 *cm* in diameter, the power supply has a voltage of 12-*Volt* (DC) and a current of 10 *A*, and varying coil length. Table 6 shows the effect of the coil length to the magnetic field force. It is worthwhile mentioning that no attraction occurred when 10 *m* coil length was used which means that the electrical magnetic force is not enough for attracting the Fe_3O_4 nanoparticles. Moreover, at 30 *m* length the Fe_3O_4 nanoparticles were attracted while the coil was started to be heated due to high power supply current which means the coil resistance is not enough. Remarkably, run number three represents the selected design parameter.

Table 6. The result of optimizing the electrical magnetic field parameters.

Runs	Coil length (m)	Result
1	10	Not Effective
2	30	Effective with side effect
3	50	Effective without side effect

Nevertheless, for futuristic industrial scale up of such in-house built prototype, Table 7 lists the major components along with the process description and the cost for each element indicating the feasibility of such nonconventional treatment process.

Table 7. Major element items, process description, and cost estimation for the prototype.

Element	Descriptions	Capital Cost ($)
Fiber Glass Cylinders	Four transparent fiberglass cylinders were used, and all of them were equipped with an opening to atmosphere. The first cylinder (pre-treatment storage cylinder) has the largest volume which is 1,500 ml of 10 cm diameter and 20 cm height. The other three-stages-treatment cylinders have smaller volume of 1,100 ml with 10 cm diameter and 15 cm height.	80
Piping system and Valves	A transparent polyethylene pipe of 16 mm diameter was used to allow visual observation of flowing water from one cylinder to another. Five manual gate valves of 16 mm diameter were installed at the entering, bottom side for each cylinder, and at the exit.	10
DC Motor	Three DC motors were installed and each one has a shaft diameter of 0.65 cm and rotates at constant speed up to 400 rpm.	90
Bearing	Six bearings were used in this design. Two bearings were mounted at each shaft to prevent vibration forms due to shaft rotation. The bearing has inner diameter of 1.2 cm.	
Couplers	Three couplers were used to connect the motor shaft with the mixer shaft.	45
Pump	Hydrostatic pump with capacity of 1 mL/sec.	25
Magnet	Three magnets were installed at the bottom of each treatment cylinders. Each magnet consists of 50 meters cupper coil wrapped around a steel rod which has dimension of 1.4 cm in diameter and 7 cm in length. Moreover, 12-volt DC power supply that provides a current of 10-A was connected in series with the magnet.	30
Mixer	Three mixers were used in this design. Each mixer shaft has diameter of 1.2 cm and varying lengths equal to 45, 50, and 65 cm.	25
Power supply	12-Volt DC power supply and current of 3.2 A	10
Boost	Intended to increase voltage which in turn increase the motor rotational speed.	10
Arduino and relays	Used to control mixers and magnets start-stop automatically.	100
Fe_3O_4	In-house prepared nanoparticles	110/1kg
H_2O_2 agent	Locally available (960 ml was used)	25/1L
Wood stand	Holding the whole setup	45
	Total ($)	605

5. Conclusions

Industrial and domestic sectors are in critical needs for emerging technologies for water and wastewater treatment. Herein, the results of this study promote the effectiveness of using magnetite (Fe_3O_4) nanoparticles within a continuous treatment process. In fact, these nanoparticles showed high efficiency and durability along with sodium persulfate ($Na_2S_2O_8$) oxidation agent for treating synthetic aqueous solution for many adsorptions and AOP cycles. This study showed the proof of concept, therefore, futuristics efforts will focus on the reaction kinetics, nanocatalysts sustainability, and synergistic effects upon using different competitive model molecules in the water matrix within a fully automated and modified prototype.

Acknowledgments

The authors would like to thank the Mechanical and Chemical Engineering Departments at An-Najah National University for providing access to their labs for the experimental works.

Funding

None.

Declarations

Conflict of interest Authors declare that they have no conflict of interest.

References

[1] Ribeiro, A. R.;Nunes, O. C.;Pereira, M. F.; Silva, A. M. An overview on the advanced oxidation processes applied for the treatment of water pollutants defined in the recently launched Directive 2013/39/EU. *Environment International* **2015**, *75*, 33-51.

[2] Paździor, K.;Bilińska, L.; Ledakowicz, S. A review of the existing and emerging technologies in the combination of AOPs and biological processes in industrial textile wastewater treatment. *Chemical Engineering Journal* **2019**, *376*, 120597.

[3] Bilińska, L.;Blus, K.;Gmurek, M.; Ledakowicz, S. Coupling of electrocoagulation and ozone treatment for textile wastewater reuse. *Chemical Engineering Journal* **2019**, *358*, 992-1001.

[4] Husam, A.-N.; Nassar, A. Slaughterhouses wastewater characteristics in the Gaza strip. *Journal of Water Resource Protection* **2019**, *11*, 844.

[5] Nassar, N. N.;Marei, N. N.;Vitale, G.; Arar, L. A. Adsorptive removal of dyes from synthetic and real textile wastewater using magnetic iron oxide nanoparticles: thermodynamic and mechanistic insights. *The Canadian Journal of Chemical Engineering* **2015**, *93*, 1965-1974.

[6] Ramallah Palestinian Central Bureau of Statistics. *Palestine Localities, Bitunia* **2016**.

[7] Yang, Q.;Ma, Y.;Chen, F.;Yao, F.;Sun, J.;Wang, S.;Yi, K.;Hou, L.;Li, X.; Wang, D. Recent advances in photo-activated sulfate radical-advanced oxidation process (SR-AOP) for refractory organic pollutants removal in water. *Chemical Engineering Journal* **2019**, *378*, 122149.

[8] Andreozzi, R.;Caprio, V.;Insola, A.; Marotta, R. Advanced oxidation processes (AOP) for water purification and recovery. *Catalysis Today* **1999**, *53*, 51-59.

[9] Amde, M.;Liu, J.-f.;Tan, Z.-Q.; Bekana, D. Transformation and bioavailability of metal oxide nanoparticles in aquatic and terrestrial environments. A review. *Environmental pollution* **2017**, *230*, 250-267.

[10] Rai, P. K.;Kumar, V.;Lee, S.;Raza, N.;Kim, K.-H.;Ok, Y. S.; Tsang, D. C. Nanoparticle-plant interaction: Implications in energy, environment, and agriculture. *Environment international* **2018**, *119*, 1-19.

[11] Zu, D.;Wang, H.;Lin, S.;Ou, G.;Wei, H.;Sun, S.; Wu, H. Oxygen-deficient metal oxides: Synthesis routes and applications in energy and environment. *Nano Research* **2019**, *12*, 2150-2163.

[12] Alsurakji, I. H.;El-Qanni, A.;El-Hamouz, A. M.;Warad, I.; Odeh, Y. Thermogravimetric Kinetics Study of Scrap Tires Pyrolysis Using Silica Embedded With NiO and/or MgO Nanocatalysts. *Journal of Energy Resources Technology* **2021**, *143*, 092302.

[13] Xu, P.;Zeng, G. M.;Huang, D. L.;Feng, C. L.;Hu, S.;Zhao, M. H.;Lai, C.;Wei, Z.;Huang, C.; Xie, G. X. Use of iron oxide nanomaterials in wastewater treatment: a review. *Science of the Total Environment* **2012**, *424*, 1-10.

[14] Hung, C.-M.;Chen, C.-W.;Jhuang, Y.-Z.; Dong, C.-D. Fe_3O_4 magnetic nanoparticles: characterization and performance exemplified by the degradation of methylene blue in the presence of persulfate. *Journal of Advanced Oxidation Technologies* **2016**, *19*, 43-51.